Atherosclerotic Plaque Motion Trajectory Analysis from Ultrasound Videos

S. E. Murillo[1], M. S. Pattichis[1], C. P. Loizou[2], C. S. Pattichis[3], E. Kyriacou[4],
A. G. Constantinides[5] and A. Nicolaides[6]

[1]Dept. of ECE, University of New Mexico, Albuquerque, NM-87131, USA, {smurillo, pattichis}@ece.unm.edu
[2]Dept. of CS, Intercollege, CY-3507 Limassol, Cyprus, christosl@lim.Intercollege.ac.cy
[3]Dept. of CS, University of Cyprus, CY1678 Nicosia, Cyprus, pattichi@ucy.ac.cy
[4]Cyprus Institute of Neurology and Genetics, CY1683, Nicosia, Cyprus, ekyriac@ucy.ac.cy
[5]Department of Electrical and Electronic Engineering, Imperial College, a.constantinides@imperial.ac.uk
[6]Imperial College, London, England, Univ. of Cyprus and Vascular Screening and Diagnostic Centre, Nicosia, Cyprus, anicolai@cytanet.com.cy

Abstract— The paper describes the computation of motion trajectories in ultrasound videos of atherosclerotic plaques. Preliminary results indicate that motion trajectories follow the cardiac cycles, forcing motions from different parts of the plaque and arterial walls to appear in phase. Based on the periodicity of the motion, we found that a Fourier series, using a small number of harmonics, can approximate the periodic motion due to the cardiac motion cycle. Furthermore, plaque motion exhibited larger deviations and more abrupt changes than arterial wall motion.

Index Terms— **Atherosclerosis, motion estimation, ultrasound, carotid plaque.**

I. INTRODUCTION

Carotid atherosclerosis is the primary cause of stroke and the third leading cause of death in the United States. Almost twice as many people die from cardiovascular diseases than from all forms of cancer combined. Atherosclerosis is a disease of the large and medium size arteries, and it is characterized by plaque formation due to progressive intimal accumulation of lipid, protein, and cholesterol esters in the blood vessel wall [1], which reduces blood flow significantly. Traditionally the degree of artery stenosis, or narrowing, has been targeted as the marker for assessment of risk for plaque vulnerability depended on the type of plaque, and considered to cause either a complete arterial occlusion or ischemic event in the brain. The risk of stroke increases with the severity of carotid stenosis and is reduced after carotid endarterectomy [2]. It is also anticipated that plaque and wall motion may provide additional and important information about normal or abnormal motion, measuring the plaque instability, and the degree of stenosis, thus giving indication of an individual to develop a stroke.

To the best of our knowledge there are no other studies reported in the literature, where the carotid plaque motion trajectories from ultrasound videos were investigated. In recent studies, we have shown that the quality of ultrasound carotid artery images can be improved after despeckle filtering and normalization [3], [4]. These findings may also be used for increasing the accuracy of the motion estimation algorithm. Furthermore, the accurate segmentation of the carotid plague [5] may help in reducing the size of the area of interest and thus improve the final motion estimation results.

In [6], the authors measured 3D plaque motion velocity over the plaque surface, and concluded that symptomatic plaques exhibited motion that was significantly different from motion of the internal carotid artery. Furthermore, they claimed the measured Maximal discrepant surface velocity (MDSV) for symptomatic plaques was significantly higher than the corresponding velocities for asymptomatic plaques, and also suggested that further studies were needed.

The purpose of this research is to develop verifiable methods for estimating motion trajectories in ultrasound videos of the carotid plaque. Motion trajectories are computed throughout the plaque, the plaque-arterial boundary, and the carotid artery. We examine the maximum displacements of the computed trajectories and compare motion trajectories among the different regions.

Preliminary results indicate that motion trajectories follow the cardiac cycles, forcing motions from different parts of the plaque and arterial walls to appear in phase. Furthermore, from the periodicity of the motion, a Fourier series, using a small number of harmonics, can approximate the periodic motion due to the cardiac motion cycle. It was also found that plaque motion exhibited larger deviations and more abrupt changes than arterial wall motion.

The rest of the paper is broken into three sections. In section II, we provide a summary of the proposed method. In section III, we present motion trajectory results on both synthetic are real videos. We give concluding remarks in section IV.

II. METHODS

Motion estimation relies on the use of the Horn and Schunk algorithm [7]. The basic assumption is that image intensity remains constant throughout the video. Thus, when a pixel (x, y) in frame indexed at time t moves to $(x + \delta x, y + \delta y)$ at time $t + \delta t$, we assume that:

$$I(x, y, t) = I(x + \delta x, y + \delta y, t + \delta t). \qquad (1)$$

Following a Taylor series expansion, assuming continuity in image intensity, we obtain the ill-posed, optical flow equation

$$I_x u + I_y v + I_t = 0, \qquad (2)$$

where $u(x, y), v(x, y)$ denote velocity estimates at pixel (x, y). To solve (2), we rely minimize the functional

$$\iint \left(\alpha^2 E_c^2 + E_b^2 \right) dx\, dy \qquad (3)$$

where:

$$E_b^2 = \left(I_x u + I_y v + I_t \right)^2$$

$$E_c^2 = \left(\frac{\partial u}{\partial x} \right)^2 + \left(\frac{\partial u}{\partial y} \right)^2 + \left(\frac{\partial v}{\partial x} \right)^2 + \left(\frac{\partial v}{\partial y} \right)^2 .$$

The motion estimates are then used to compute pixel motion throughout the video using an ODE solver applied to the velocity estimates.

A. Motion Trajectory Estimation Implementation

The optical-flow method for motion estimation was implemented on the Los Lobos cluster (512 Pentium III processors) of the Albuquerque High Performance Computing Center, using an MPI extension of available code. Estimates for each video frame (total=179) were computed for many different values of the parameters, and the estimates that exhibited the largest density were used. For an ODE solver, we use the explicit Runge-Kutta (4,5) formula [8] provided by Mathworks [9].

III. RESULTS

A. Results on Synthetic Data

In Fig. 1, we present results from vertical motion estimation. For the simulated motion video, we generated a synthetic motion that is in agreement with both our experience and our measurements (presented in the following sections). We assumed periodic motion at 7 cycles per total video-length (video length = 179 frames). Both motion components are set to be equal. We used three harmonics: at 7, 14, and 21 cycles per video-length to represent the motion, where each amplitude decayed at a rate that is one over the frequency. From Fourier analysis, the motion simulation represents periodicity in the time-domain, where the period is one-seventh of the video-length, while the harmonic decay assumes that the motion itself allows for discontinuities over a finite number of points. This model is in agreement with our observations of visible motion discontinuities due to sudden motion (also see results on real-video examples).
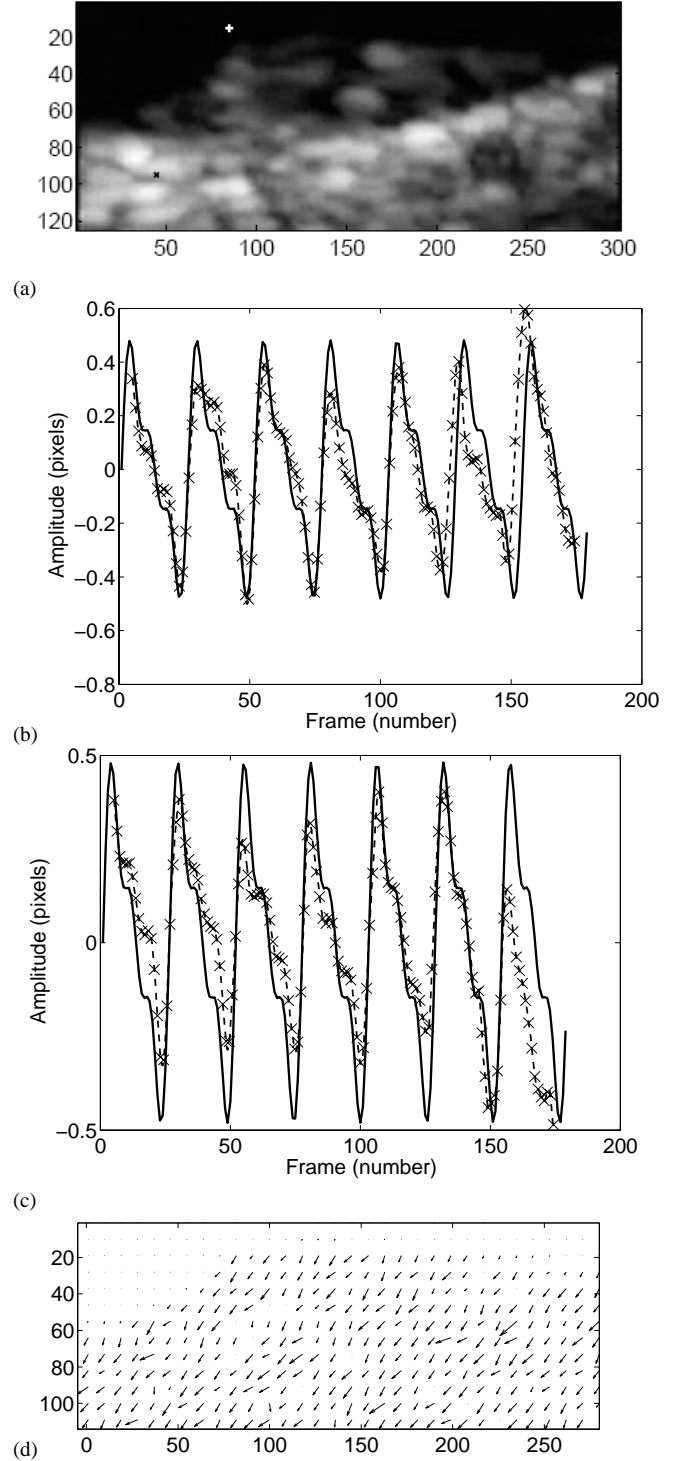

(a)

(b)

(c)

(d)

Fig. 1. Periodic plaque motion simulation: (a) original video frame used to simulate the motion, (b) vertical pixel motion at plaque-wall boundary point (row=95, column=45) with ground truth (solid line) and estimated (dotted line), (c) horizontal motion at plaque-blood boundary point (row=15, column=85), ground truth (solid line) and estimated (dotted line), and (d) motion estimates on the seventh frame of the simulated video.

In any case, clearly, if the sampling frame-rate had been dramatically improved, this motion may appear smoother. In Fig. 1(a), we show the first video frame, from which the rest of the video was generated. The rest of the video is generated

using cubic-spline interpolation from the first frame. The simulated video includes a plaque (top-portion) and the arterial wall (bottom of the video). We show results from vertical motion trajectory estimation near the plaque-wall boundary (Fig. 1(b)), at the bottom-left plaque region, horizontal motion trajectory estimation at the plaque-blood boundary (Fig. 1(c)),at the upper-left plaque region, and full motion estimation vectors over the entire video frame (Fig. 1(d)). From the results, it is clear that relatively-accurate motion estimation is possible at the plaque-wall boundary (Fig. 1(b)), but not at the plaque-blood boundary (Fig. 1(c)) where the tracking line, dashed line, presents more error following the ground truth, solid line. The estimation problem with motion-estimation over the plaque-blood boundary can be attributed to motion estimation issues over this discontinuous-boundary. As it is clear from Fig. 1(d), we can also see that we have edge artifacts and speckle noise, forcing unreliable estimates over the edge boundaries.

B. Results on videos of the Carotid Plaque

We present motion trajectory results from two real-video examples. The results are summarized in Figs 2-5.
In Fig. 2(a), we show the first frame of the motion video, while the estimated, corresponding trajectories are shown in Fig. 2(b). In Fig. 2(b), reliable motion trajectories that span the entire video are shown. There is significant variation in the motion trajectories, as a function of the location of the initial point on the plaque or the arterial walls.
For three different points, we present vertical motion trajectories in Fig. 3. From the results, it is clear that the trajectory-estimates follow the cardiac motion cycle. This is also reinforced by the fact that all three points appear to be – approximately- in-phase. It is also shown in Fig. 3, that the variation for the first point, is higher indicating that points lying in the top region of the plaque exhibit larger movements. In Fig. 2(a), we see that vertical plaque motion appears to be decreasing in amplitude, over time. For the beginning frames, it is clear that the plaque motion exhibits the largest motion deviation. On the other hand, arterial motion appears to be less, reflecting the more stable nature of the arteries. It is also interesting to note that the DFT spectra of the motion show that the plaque motion trajectory contains stronger, high-frequency components. This observation appears to hold for our second video example shown in Figs. 4 and 5. In the second real-video example, it is also clear that plaque motion is of significantly larger amplitude than arterial motion (see Fig. 5(a)). It is also clear in Fig. 5(a) that plaque point motion is characterized by sharp changes.
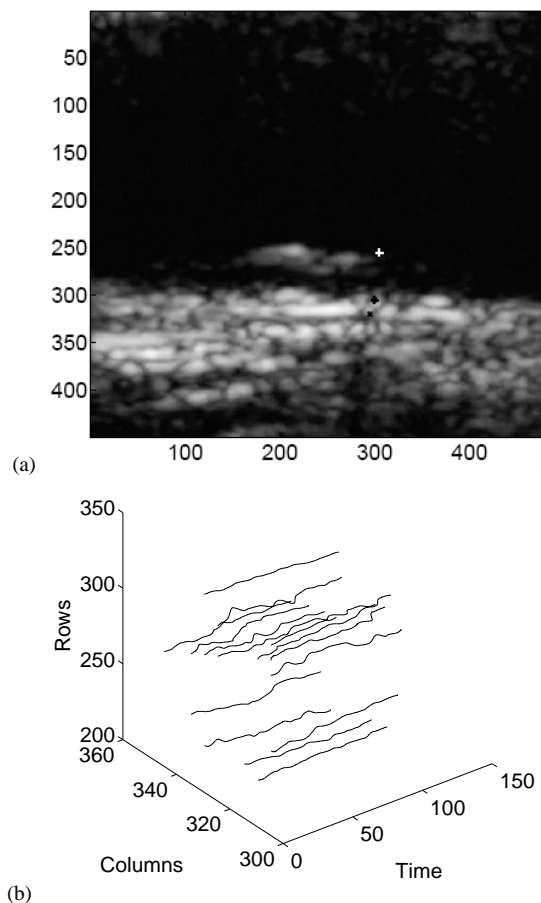

(a)

(b)

Fig. 2. First video motion estimation example: (a) first video frame shown. with plaque on the far wall of the carotid artery, and (b) 3D motion trajectory plots for different points on the right side of the plaque and arterial wall.

IV. CONCLUSION AND FUTURE WORK

Our preliminary findings suggest that we maybe able to measure plaque instability in terms of the motion trajectories of points on the plaque.

Our research is now focused on several extensions of the reported research. First, we are interested in understanding the performance of the motion estimation algorithms in the presence of speckle noise. We will then employ de-speckle filtering [4] to reduce the speckle noise and edge artifacts and hopefully improve motion trajectory estimation. Secondly, we are looking at the use of the divergence of the velocity estimates as a measure of local deformation of plaque morphology. Thirdly, we want to investigate the use of other motion estimation methods for improving trajectory estimation. Finally, we will apply an accurate automated segmentation method [5], for exactly estimating the plaque borders, which will significantly reduce the computational time and improve the final motion estimation outcome.
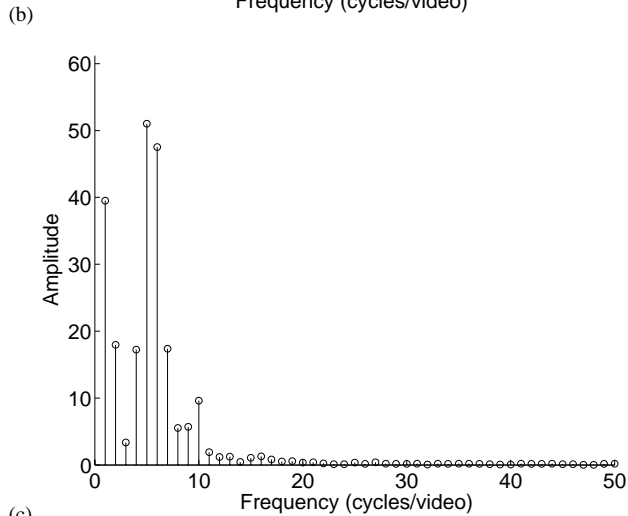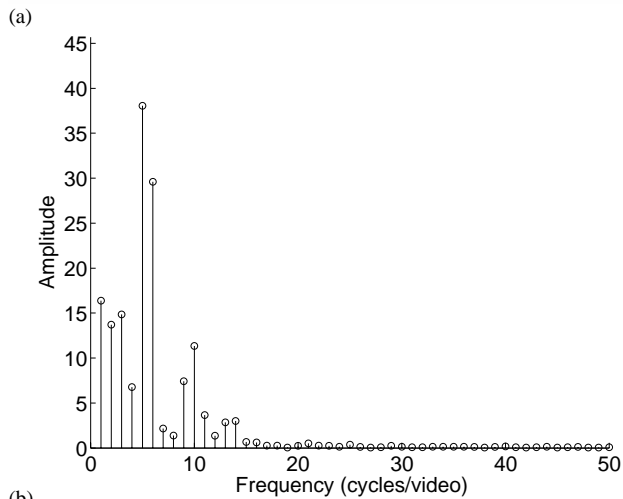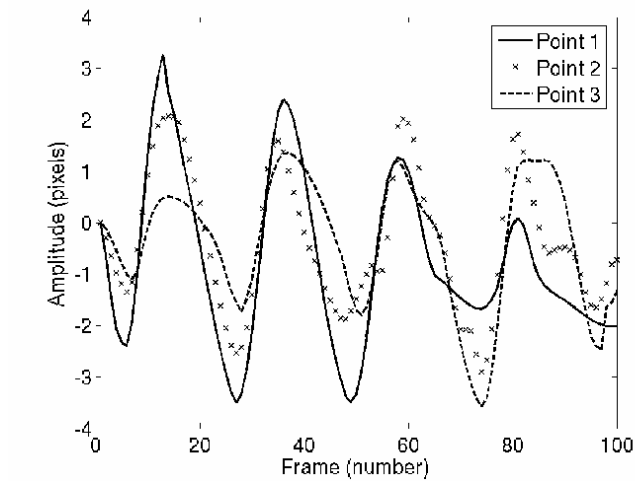
(a)

(b)

(c)

Fig. 3. Vertical motion trajectory plots for first plaque-video example: (a) vertical displacement plots for points: top-plaque point (row=255, column=305 ,plaque-wall boundary point (row=305, column=300) and wall-point (row=320, column=295) respectively, (b) Windowed-DFT plot for (row=255, column=305), (c) Windowed-DFT plot for (row=320, column=295).
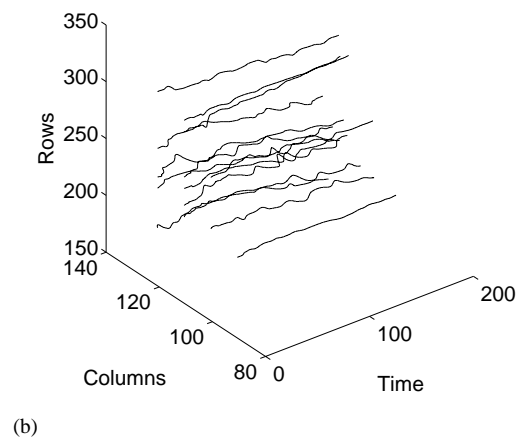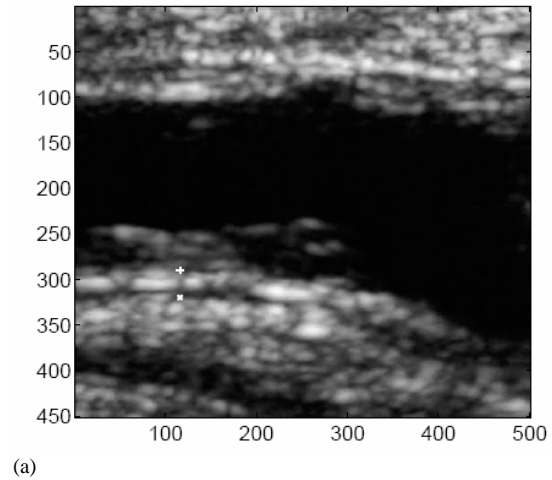

(a)

(b)

Fig. 4. Second video motion estimation example: (a) first video frame shown, with plaque (again) on the far wall of the carotid artery, and (b) 3D motion trajectory plots for different points on the left side of the plaque and arterial wall.

REFERENCES

[1] C.K. Zarins, C. Xu, Glagov S., "Atherosclerotic Enlargement of the Human Abdominal Aorta," (Elsevier Sc. Ireland), pp.157-164, 1995.

[2] ACAS clinical advisory, "Carotid Endarterectomy for Patients with Asymptomatic Internal Carotid Artery Stenosis," *Stroke*, vol. 25, no. 12, pp. 2523-2524, 1994.

[3] C.P. Loizou, C.S. Pattichis, M. Pantziaris, T. Tyllis, A. Nicolaides, "Quantitative Quality Evaluation of Ultrasound Imaging in the Carotid Artery," *Med. Biol. Eng. Comput.*," vol. 44, no. 5, pp. 414-426, 2006.

[4] C.P. Loizou, C.S. Pattichis, C.I. Christodoulou, R.S.H. Istepanian, M. Pantziaris, A. Nicolaides "Comparative Evaluation of Despeckle Filtering in Ultrasound Imaging of the Carotid Artery," *IEEE Trans. Ultrasonics Ferroelectrics and Frequency Control*, vol. 52, no. 10, pp. 1653-1669, 2005.

[5] C.P. Loizou, C.S. Pattichis, R.S.H. Istepanian, M. Pantziaris, A. Nicolaides, "Atherosclerotic Carotid Plaque Segmentation," *Proc. Of the 26th Annual Int. Conf. IEEE EMBS,* San Francisco, California, USA, Sept. 1-5, pp. 1403-1406, 2004.

[6] S. Meairs and M. Hennerici, "Four-dimensional ultrasonographic characterization of plaque surface motion in patients with symptomatic and asymptomatic carotid artery stenosis," *Stroke*, vol. 30, no. 9, pp. 1807-1813, Sep. 1999.

[7] B. K.P. Horn and B. G. Schunck, "Determining Optical Flow," *Artificial Intelligence*, vol. 17, pp. 185-203, 1981.

[8] J. R. Dormand and P. J. Prince, "A family of embedded Runge-Kutta formulae," *J. Comp. Appl. Math.*, vol. 6, pp 19-26, 1980.

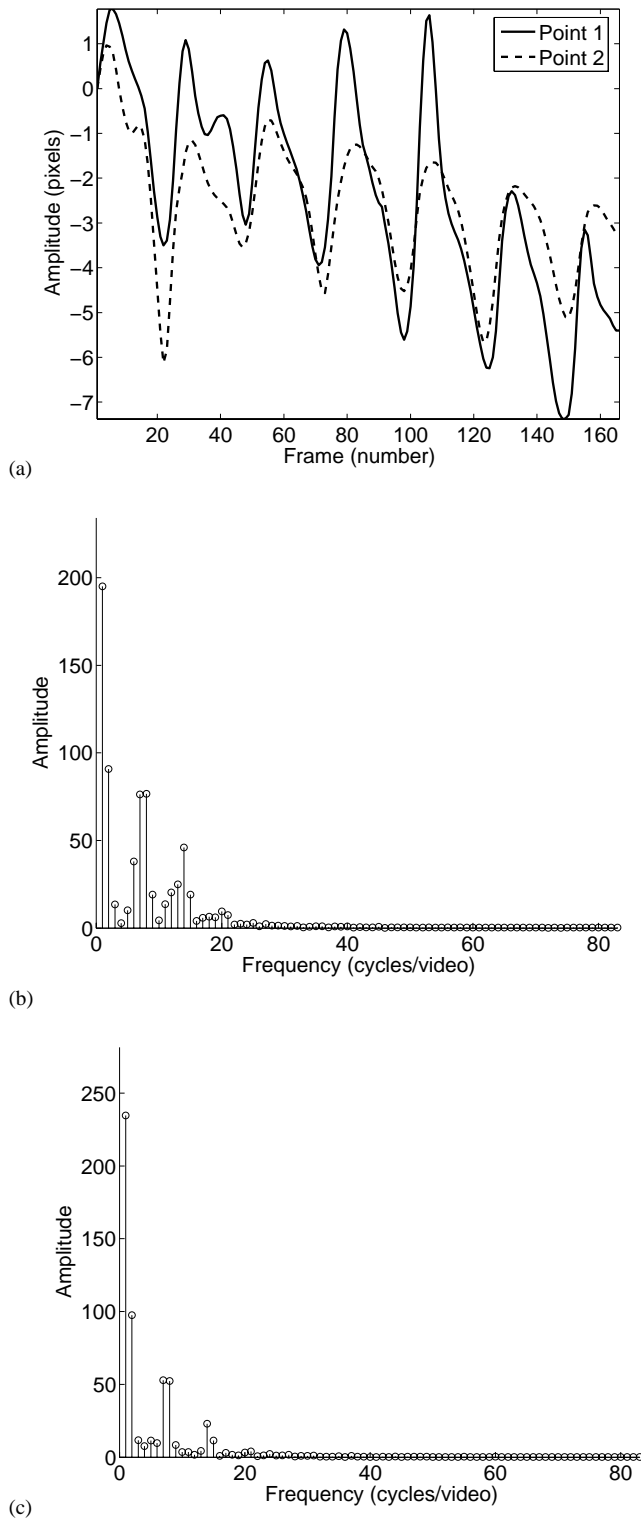[9] Web link: http://www.mathworks.com.

(a)

(b)

(c)

Fig. 5. Vertical motion trajectory plots for second plaque-video example: (a) vertical displacement plots for two points: bottom-mid-plaque point (row=290, column=116), plaque-wall boundary point (row=320, column=116) respectively, (b) Windowed-DFT plot for (row=290, column=116), (c) Windowed-DFT plot for (row=320, column=116). Note the DFT amplitude peaks at 7 and 14 cycles/video-length.